PROCEEDINGS of the
23rd International Congress on Acoustics

9 to 13 September 2019 in Aachen, Germany

Guided Lamb and edge wave excitation by piezoelectric transducers in elastic plates

Mikhail V. GOLUB[1]; Artem A. EREMIN[2]; Maria V. WILDE[3]; Alisa N. SHPAK[4]; Inka MUELLER[5]

[1,2,4] Institute for Mathematics, Mechanics and Informatics, Kuban State University, Russian Federation

[3] Faculty of Mathematics and Mechanics, Saratov State University, Russian Federation

[5] Department of Civil and Environmental Engineering, Ruhr-University Bochum, Germany

ABSTRACT

In this contribution, the results of theoretical and experimental studies of guided waves excitation by piezoelectric transducers attached at an edge or a face of an elastic plate are reported. The semi-analytical methods relying on integral transform and modal expansion techniques are applied for numerical analysis. Wave energy distribution amongst excited guided waves (Lamb and edge waves) is carefully analysed and discussed to improve the quality of damage identification with techniques based on guided waves. The influence of partial debonding of a piezoelectric transducer on guided waves excitation is investigated. The potential of edge waves for practical applications in non-destructive evaluation and structural health monitoring is discussed. Namely, it is demonstrated that edge waves excited in plates and scattered by surface-breaking cracks can be useful for detection of defects located at the edges.

Keywords: Guided waves, Edge wave, Lamb wave, Piezoelectric transducer, Wave excitation

1. INTRODUCTION

Elastic guided waves (GWs) are widely employed in ultrasonic NDT/NDE for damage characterization due to their capabilities for long-range propagation and sensitivity to defects. For excitation and sensing of GWs, thin piezoelectric transducers adhesively attached to the structure are among commonly utilized tools [1]. Debonding or imperfect contact between a transducer and an inspected structure can result in the failure of the whole SHM system. Thus, the objective of the monitoring applies to the piezoelectric wafer active sensors (PWASs) as well [2]. The complexity of wave propagation and excitation in laminates conditioned by, e.g., the multimodality of GW motion, dynamics of piezoelectric transducers and the quality of their contact with the host structure should be properly addressed for better performance of GW-based NDT/NDE systems. The aim of the present study is to apply semi-analytical mathematical approaches in order to study Lamb wave excitation by fully bonded and partially debonded piezoelectric transducers in plates. The potential of GWs propagating along plate edges for practical applications is discussed and experimentally justified.

2. MATHEMATICAL MODELLING

2.1 Guided waves

To consider wave propagation in an elastic plate of thickness H, let us introduce the Cartesian coordinates as shown in Figure 1. Two locations of PWAS for GW generation are considered: a rectangular PWAS with dimensions 30 mm x 5 mm x 0.25 mm adhesively attached to the face and at the edge of the plate (see Figure 1). In the numerical simulations, vibrations of an elastic plate are

[1] m_golub@inbox.ru
[2] eremin_a_87@mail.ru
[3] mv_wilde@mail.ru
[4] alisashpak7@gmail.com
[5] inka.mueller@aol.de

described by the Lame equations of the linear theory of elasticity, which are formulated in terms of the displacement vector, while vibrations of the piezoelectric transducer are expressed in terms of the displacement vector and the electric potential (for more details see [3]). The faces of the plate except the contact area S_c between the PWAS and the plate (bottom of the PWAS in this case), where the continuity of traction and displacement vectors is assumed, are modelled via stress-free boundary conditions. If the PWAS is partially debonded, the bottom of the PWAS is split into two parts: the contact area S_c and the debonded domain S_d, where stress-free boundary conditions are assumed. Severity C of PWAS's damage is defined as the ratio between the area of the debonded domain S_d and the total area of the bottom of the PWAS.

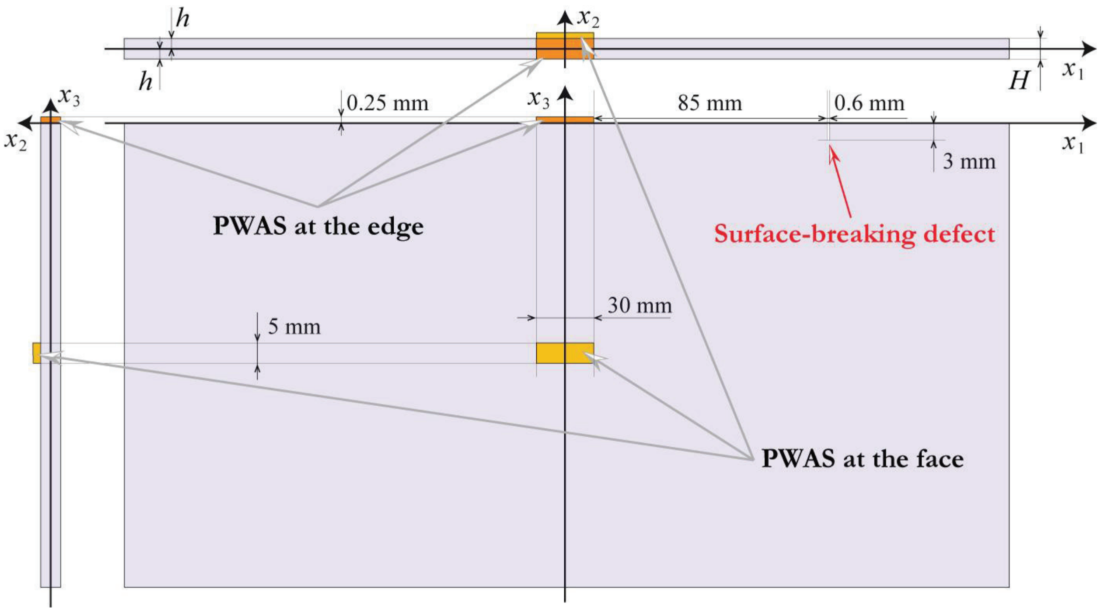

Figure 1 – Geometry of the problem considered

Along with the Lamb waves, guided edge waves (EW) can propagate in elastic plate shown in Figure 1 [4,5]. Figure 2 demonstrates slownesses of propagating GWs (both, LWs and EWs) in a rectangular aluminium elastic plate with Lame constants $\lambda = 51.1$ GPa, $\mu = 26.3$ GPa and mass density $\rho = 2640$ kg/m^3. At lower frequencies, the wave energy generated by a PWAS mounted at a surface is to be distributed among two fundamental Lamb waves ($A0$ and $S0$), two fundamental EWs ($EA0$ and $ES0$) and $SH0$.

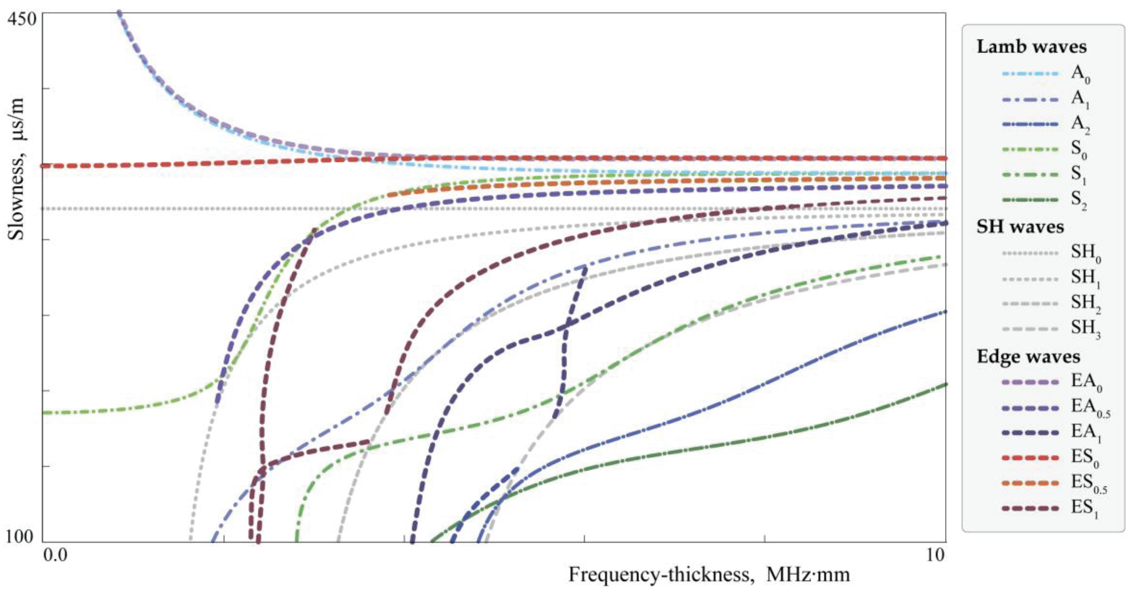

Figure 2 – Slownesses of GWs propagating in an aluminium plate

2.2 Transducer at the face of an elastic plate

Dynamic interaction of a PWAS attached to a face of an elastic plate (PWAS centre is situated at $(0, h, -b)$) is simulated within the plane-strain assumption, i.e., a two-dimensional model is considered. It is based on the semi-analytical hybrid approach (SAHA) [3], which employs the boundary integral equation method [4] and the spectral element method [5]. According to the SAHA, the displacement vector and the electric potential function in the PWAS are expanded with Lagrange interpolation polynomials at Gauss–Lobatto–Legendre points. These expansions are substituted into the equations of motion, the latter leads to the corresponding system of linear algebraic equations. The semi-analytic nature of the SAHA enables to extract GWs from the total wave-field and, therefore to analyse energy distribution among GW propagation in different directions from the source of motion. It should be mentioned that the SAHA can be applied to simulate guided waves scattered by defects.

In order to model dynamic interaction of the piezoelectric transducer with the plate, continuity of the displacements and stresses in the contact area is assumed. The traction vector-function is interpolated with the splines and the solution is found in the nodal points. If the degradation of the contact (debonding) is to be modelled, the traction vector function is assumed zero at the nodal points belonging the area of debonding and, therefore, the continuity condition is disregarded. Detailed description of the proposed mathematical method is given in [3].

Since the two-dimensional model is applied, only the following wave energy distribution coefficients can be defined:

$$\eta_m^{\pm} = E_m^{\pm} / E^{(0)}. \tag{1}$$

Here $E^{(0)}$ is the whole amount of wave energy transferred by the PWAS along the x_1 axis into the plate, whereas $E_m^{\pm}$ denotes the wave energy carried by m-th Lamb wave in the directions $x_3 \to \pm\infty$. The amount of wave energy is determined in terms of the time-averaged power density vector or Umov-Poynting vector [6]

$$e_j = -\frac{\omega}{2} \mathrm{Im}\left(\sum_{i=1}^{3} u_i \sigma_{ij}^* \right). \tag{2}$$

In the case of the PWAS attached at the face of the plate, the following expressions are employed:

$$\begin{gathered} E^{(0)} = -\int_{-h}^{h} \int_{-l/2}^{l/2} e_3(x_1, 0, x_3) dx_1 dx_3, \\ E_m^{\pm} = \iint_{S_R} (\mathbf{e} \cdot \mathbf{n}) dS, \quad S_R^{\pm} = \{(x_3 - b)^2 + x_1^2 = R^2, -h \le x_2 \le h, x_3 \gtrless b\}. \end{gathered} \tag{4}$$

If the PWAS is perfectly bonded, the wave-fields excited by the PWAS are symmetric with respect to the x_3 axis, so $E_m^+ = E_m^-$ and distribution coefficients $\eta_m = \eta_m^+ + \eta_m^-$ are more applicable. It should be also noted that only Lamb wave excitation is studied within the model described since the PWAS is located far from the edges, where EW can propagate.

2.3 Transducer at the edge of elastic plate

In [6], the semi-analytical method based on the application of the Fourier transform with the modal expansion of the displacement vector was applied to describe the GW excitation in the plate with the PWAS attached at the edge $x_3 = 0$. This method is employed in the study to calculate the wave energy distribution coefficients $\eta_m = E_m / E^{(0)}$ defined via

$$E^{(0)} = -\int_{-h}^{h} \int_{-l/2}^{l/2} e_3(x_1, x_2, 0) dx_1 dx_2, \quad E_m = \iint_{S_R} (\mathbf{e} \cdot \mathbf{n}) dS, \quad S_R = \{x_3^2 + x_1^2 = R^2, -h \le x_2 \le h\} \tag{3}$$

The ratio of EWs in the spectrum is of the greatest interest here since it is important to understand how effectively EWs can be excited by piezoelectric transducers.

3. GUIDED WAVES EXCITATION BY TRANSDUCER AT THE FACE

To analyse the influence of the bonding conditions between the PWAS and the waveguide on the energy distribution among GWs, wave energy distribution coefficients η_m are used. Figures 3-6 demonstrate the influence of the frequency on η_m showing ratio of the m-th mode in $E^{(0)}$. The simulation have been performed for the aluminium plate of width H=4.85 mm with the PWAS (PIC 155 PI Ceramics) of 5 mm width and 0.25 mm height, while Figure 7 shows the variation of the amount of energy transferred into the waveguide for all the cases considered in Figures 3-6. Figure 3 demonstrates the alteration of η_m if the PWAS is debonded in the middle and the edges are still glued. It is observed that relatively small debonding (C=20 %) in the middle (Figure 3c) has almost no influence on the wave energy distribution. The changes due to debonding are also not very substantial at higher frequencies. With the debonding area growth, the energy distribution changes significantly. Moreover, a number of extra sharp resonance peaks are visible in η_m and $E^{(0)}$ plots for severer debonded PWASs (Figures 3b and 3d).

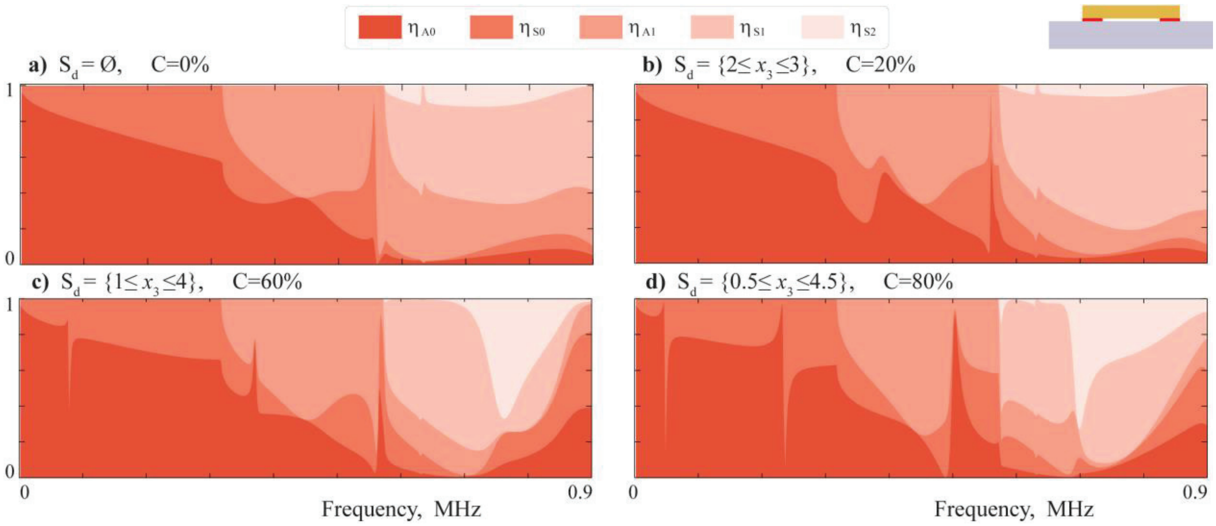

Figure 3 – Wave energy distribution coefficients η_m for PWASs with symmetric debonding in the centre

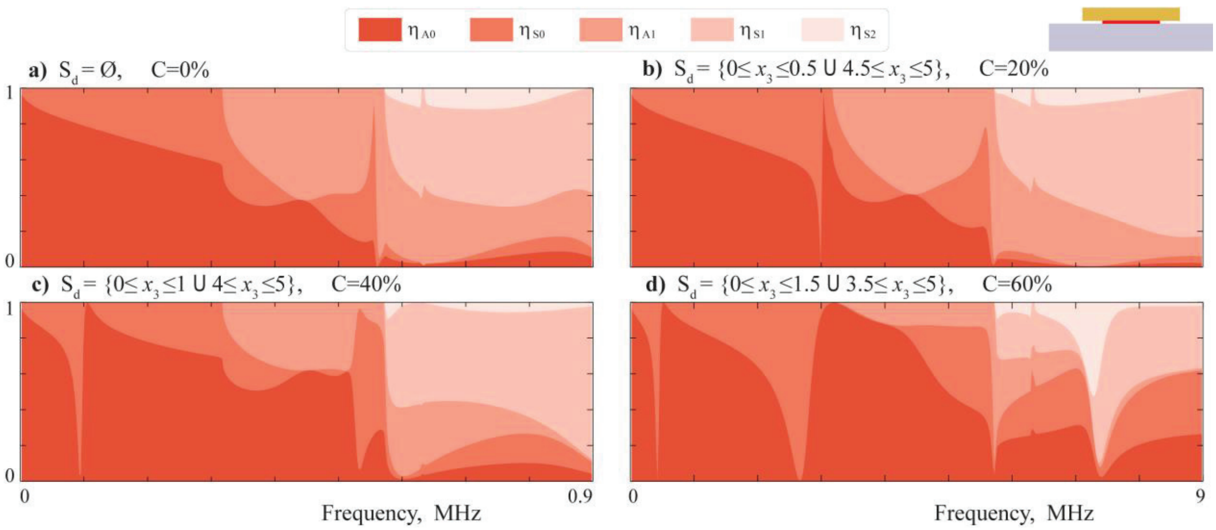

Figure 4 – Wave energy distribution coefficients η_m for two-sided symmetrically debonded PWASs

Figure 4 depicts wave energy distribution coefficient dependence on the debonding area S_d of two edges of the PWAS are symmetrically debonded, while the middle part is glued. One can observe that even small debonding of the edges (0.5 mm from each edge – Figure 4b) alters energy distribution close to the frequency f=300 kHz, where a sharp peak is visible in $E^{(0)}$ plot. At this frequency, the energy distribution of the perfectly glued PWAS $\eta_{A0}:\eta_{S0}$=65:35 but if the 0.5 mm of the bottom surface are not properly glued, the energy distribution changes to $\eta_{A0}:\eta_{S0}$=5:95.

If debonding of a PWAS is asymmetric, amount of energy transferred in the directions $x_3 \to \pm\infty$ are different. The energy distribution among Lamb waves excited by PWASs with one-sided asymmetric debonding is shown at the Figure 5. As expected, for the majority of frequencies more wave energy is transferred to the side, where the PWAS is bonded. Additionally, sharp peaks corresponding to the abrupt alteration in the modes' distribution are visible and the number of the peaks increases with the debonding area growth.

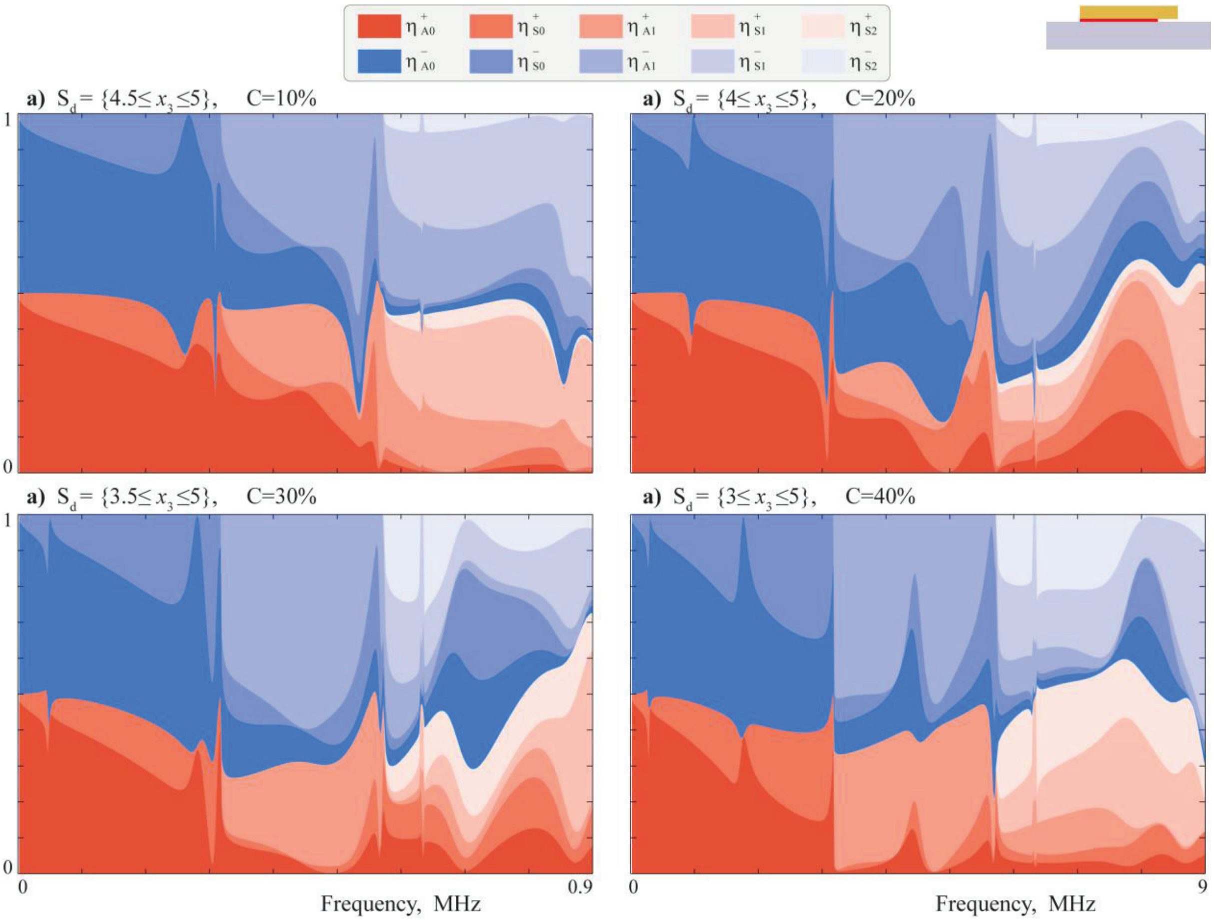

Figure 5 – Wave energy distribution coefficients $\eta_m^{\pm}$ for one-side debonded PWASs

Distribution of the energy excited by PWASs with two-sided asymmetric debonding is demonstrated in Figure 6. An interesting effect is observed in a narrow frequency range around f=295 kHz, which is right below the cut-off frequency of A1 mode. In this frequency range, the amount of energy E_m^{+} carried by Lamb waves in the positive direction abruptly increases and exceeds E_m^{-}. It is also visible that at lower frequencies (up to 200 kHz) $A0$ mode prevails in the excited wave-field for debonded PWASs except for the areas near resonance frequencies.

Analysis of Figures 3-6 allows concluding that defect in contact zone between the PWAS and the waveguide can cause significant changes in wave excitation even if the damaged zone is not large (C<20%). Debondings may alter amount of energy and its distribution among Lamb waves substantially, especially if debonding is asymmetric. Nevertheless, if the defect does not touch edges of the PWAS (i.e. edges of the PWAS are glued properly) this debonding causes changes at higher frequencies. Even in this case, there are frequencies close to the resonance, where the energy distribution alters significantly compared to the perfectly glued PWAS case.

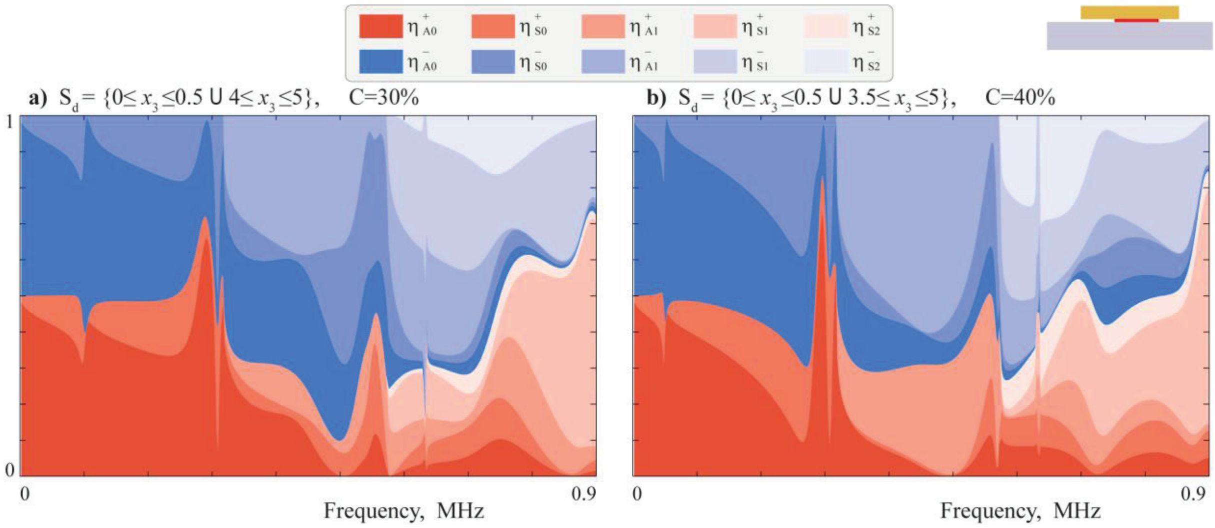

Figure 6 – Wave energy distribution $\eta_m^{\pm}$ for two-sided asymmetrically debonded PWASs

Figure 7 presents the dependence of the excited energy E^0 on the frequency if PWAS is debonded. Energy plots shown at Figure 7a, 7b, 7c and 7d are calculated for the same contact conditions as considered in Figures 3,4, 5 and 6 respectively. Alteration in the contact conditions leads to the appearance of additional maxima of in $E^{(0)}$ plots, (initial maxima remain intact at the same frequency, though absolute value of $E^{(0)}$ changes). Accordingly, all the maxima for defectively bonded PWASs are shifted to lower frequencies compared to the perfectly glued PWAS the maximum at f=580 kHz.

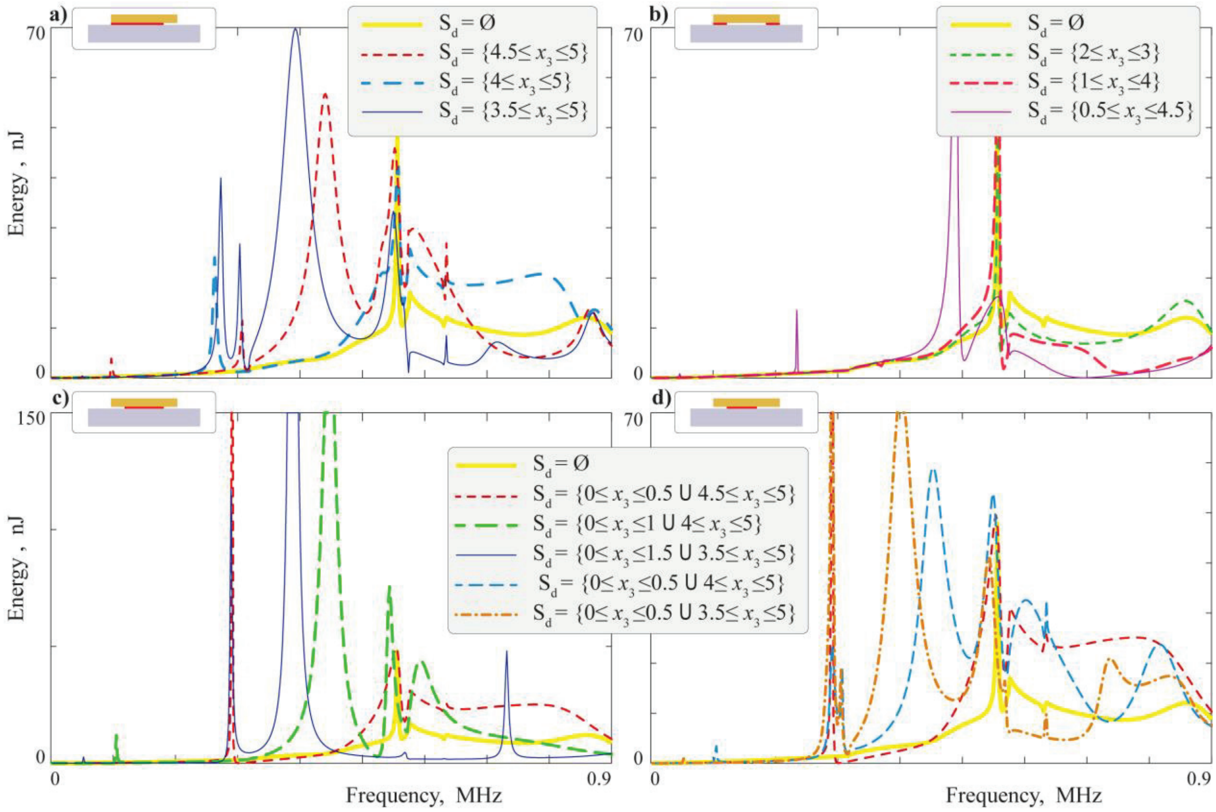

Figure 7 – Wave energy for partially debonded PWASs

4. GUIDED WAVES EXCITATION BY TRANSDUCER AT THE EDGE

In order to demonstrate importance of EW for SHM and NDE, EW and LW interaction with a surface-breaking defect at the edge of aluminium plate (notch 3 mm depth and 0.6 mm width) has been investigated experimentally. The geometry of the specimen is shown in Figure 1. The PWAS at the edge has driven with a transient voltage in the form of a narrow-band Hann-windowed five-cycle sine burst with central frequency f_0. The latter are generated by a Tektronix AFG 3022B arbitrary signal generator and are pre-amplified to the range 37.5 V-pp by a NF HSA4101 external high-frequency power amplifier before being applied to the PWAS. The out-of-plane velocities were measured by means of a Polytec PSV-500 one-dimensional scanning laser Doppler vibrometer.

It was demonstrated in [5] that fundamental mode ES0 is predominant at the edge if a PWAS is attached at the edge. Mode ES0 is not localized in the vicinity of the edge surface at lower frequencies, and the amplitudes of ES0 decay faster with depth at higher frequencies. Accordingly, relatively low reflection by surface-breaking defects is observed at central frequencies above f_0=150 kHz. Nevertheless, at the central frequencies above 200 kHz, scattering of EW becomes much stronger (more details can be found in [5,8]). In Figure 8, an example of such scattering is demonstrated for f_0=300 kHz. Figure 8 shows snapshots of the Hilbert-enveloped out-of-plane velocities $w = \partial u_2(x_1,h,x_3,t)/\partial t$ measured on the face $x_2=h$ of the specimen. It can be seen that the crack mainly reflects ES0 mode backward and reradiates it into Lamb waves. Transmitted ES0 waves are of much lower amplitudes compared to the reflected ES0 waves. Therefore, EWs provide enough information about presence of a surface-breaking defect for its identification.

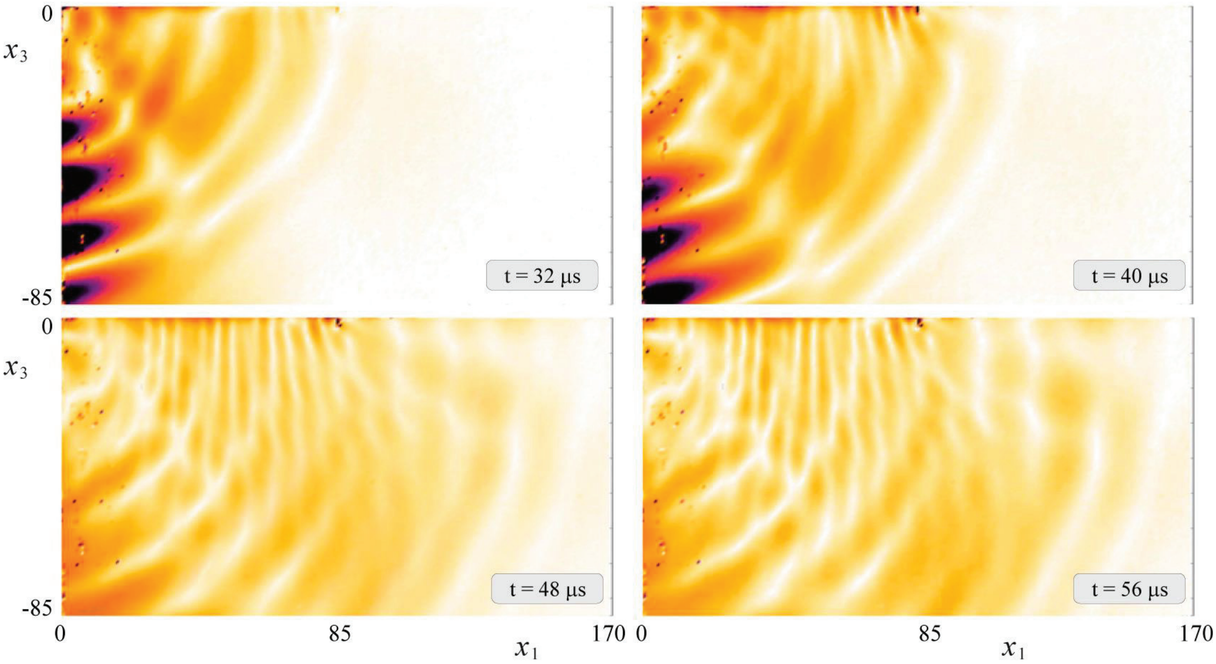

Figure 8 –Hilbert-enveloped out-of-plane velocities measured on the surface of the plate with defect of depth d=3 mm at central frequency 300 kHz at different moments of time t

5. CONCLUSIONS

A detailed analysis of Lamb waves excitation by perfectly bonded and partially debonded piezoelectric wafer active sensors has been performed. The provided analysis shows the influence of debonding between the PWAS and the structure on Lamb wave excitation. The present study also demonstrates that EW scattering by surface-breaking cracks can be used in GW-based NDT/NDE systems. Laser Doppler vibrometry is employed to approve the developed mathematical models experimentally. The authors believe that the results might be useful for practical applications.

ACKNOWLEDGEMENTS

The work is supported by the Ministry of Science and Higher Education of the Russian Federation (Project 9.1022.2017/4.6). The authors are thankful to Prof. Rolf Lammering (Institute of Mechanics, Helmut Schmidt University, Hamburg, Germany) for the comprehensive support of the experimental investigations.

REFERENCES

1. Giurgiutiu V. Structural Health Monitoring with Piezoelectric Wafer Active Sensors. Second edition, Elsevier Academic Press; 2014.
2. Buethe I, Fritzen CP. Sensor performance assessment based on a physical model and impedance measurements, Key Eng Mat. 2013; 569-570:751-758.
3. Golub MV, Shpak AN. Semi-analytical hybrid approach for the simulation of layered waveguide with a partially debonded piezoelectric structure. J Appl Math Mech. 2002;66(1):141-149.
4. Kaplunov J, Prikazchikov DA, Rogerson GA. On three dimensional edge waves in semi-infinite isotropic plates subject to mixed face boundary conditions. J Acoust Soc Am. 2005;118:2975–2983.
5. Wilde MV, Golub MV, Eremin AA. Experimental and theoretical investigation of transient edge waves excited by a piezoelectric transducer bonded to the edge of a thick elastic plate. J Sound Vib. 2019;441:26-49.
6. Glushkov EV, Glushkova NV, Ekhlakov AV. A mathematical model of the ultrasonic detection of three-dimensional cracks, J Acoust Soc Am. 1994; 95(2):681-693.
7. Kommatitsch D, Vilotte J.-P, Vai R et al. The spectral element method for elastic wave equations application to 2-d and 3-d seismic problems. Int J Numer Meth Eng. 1999;45(9):1139-1164.
8. Golub MV, Eremin AA, Wilde MV. Experimental and theoretical investigation of edge waves propagation and scattering in a thick plate with surface-breaking crack-like defect. Proceedings of 13th European Conference on Non-destructive Testing ECNDT; 11-15 June 2018; Gothenburg, Sweden, p. 0295.